Lichy, J. H., Nagata, K., Freifeld, B. R., Enomoto, T., Field, J., Guggenheimer, A., Ikeda, J.-E., Horowitz, M. S., & Hurwitz, J. (1983) *Cold Spring Harbor Symp. Quant. Biol. 47 (Part 2)*, 731–740.
Marmur, J. (1961) *J. Mol. Biol. 3*, 208–216.
Mattern, M. R., & Painter, R. B. (1977) *Biophys. J. 19*, 117–124.
Mattern, M. R., & Painter, R. B. (1979) *Biochim. Biophys. Acta 563*, 306–312.
Onodera, K., & Sheinin, R. (1970) *J. Cell Sci. 7*, 337–355.
Pardee, A. B., Dubrow, R., Hamlin, J. L., & Kletzien, R. F. (1978) *Annu. Rev. Biochem. 47*, 715–750.
Philippe, M., Sheinin, R., & de Recondo, A. M. (1984) in *Proteins Involved in DNA Replication* (Hubscher, U., & Spadari, S., Eds.) pp 295–302, Plenum, London.
Pringle, J. R., & Hartwell, L. H. (1981) in *The Molecular Biology of the Yeast Saccharomyces: Life Cycle and Inheritance* (Strathern, J. W., Jones, E. W., & Broach, J. R., Eds.) pp 97–142, Cold Spring Harbor Laboratory, Cold Spring Harbor, NY.
Richter, A., Ozer, H. L., Des Groseillers, L., & Jolicoeur, P. (1984) *Mol. Cell. Biol. 4*, 151–159.
Setterfield, G., Sheinin, R., Dardick, I., Kiss, G., & Dubsky, M. (1978) *J. Cell Biol. 77*, 246–263.
Sheinin, R. (1966) *Virology 28*, 621–632.
Sheinin, R. (1976a) *Cell (Cambridge, Mass.) 7*, 49–57.
Sheinin, R. (1976b) *J. Virol. 17*, 692–704.
Sheinin, R. (1980) in *Nuclear and Cytoplasmic Interactions in the Cell Cycle* (Whitson, G. L., Ed.) pp 105–166, Academic Press, New York.
Sheinin, R. (1984) in *Cancer, Growth and the Cell Cycle* (Friedman, S., & Skehan, P., Eds.) pp 229–248, Humana, Clifton, NJ.
Sheinin, R., & Quinn, P. A. (1965) *Virology 26*, 73–84.
Sheinin, R., & Onodera, K. (1970) *Can. J. Biochem. 48*, 851–857.
Sheinin, R., & Guttman, S. A. (1977) *Biochim. Biophys. Acta 479*, 105–118.
Sheinin, R., & Lewis, P. N. (1980) *Somatic Cell Genet. 2*, 227–241.
Sheinin, R., Darragh, P. A., & Dubsky, M. (1977) *Can. J. Biochem. 55*, 543–547.
Sheinin, R., Darragh, P. A., & Dubsky, M. (1978a) *J. Biol. Chem. 253*, 922–926.
Sheinin, R., Humbert, J., & Pearlman, R. E. (1978b) *Annu. Rev. Biochem. 47*, 331–370.
Sheinin, R., Setterfield, G., Dardick, I., Kiss, G., & Dubsky, M. (1980) *Can. J. Biochem. 58*, 1359–1369.
Sheinin, R., Fabbro, J., & Dubsky, M. (1985a) *Intervirology 24*, 174–180.
Sheinin, R., Dubsky, M., Naismith, L., & Sigouin, J. (1985b) *Exp. Cell Res. 161*, 393–405.
Sheinin, R., Dubsky, M., Sparkuhl, J., Dardick, I., & Doane, F. W. (1986) *Cell Tissue Kinet.* (submitted for publication).
Shopsis, C., & Sheinin, R. (1976) *Biochim. Biophys. Acta 433*, 101–117.
Slater, M. L., & Ozer, H. L. (1976) *Cell (Cambridge, Mass.) 7*, 49–295.
Stich, H. F., San, R. H. C., Lam, P., Korobatnick, J., & Lo, L. (1977) in *Origin of Human Cancer* (Hiatt, H., Watson, J. D., & Winsten, J. A., Eds.) pp 1499–1512, Cold Spring Harbor Laboratory, Cold Spring Harbor, NY.
Stillman, B. W., & Tamanoi, F. (1983) *Cold Spring Harbor Symp. Quant. Biol. 47 (Part 2)*, 741–750.
Todaro, G. J., & Green, H. (1963) *J. Cell Biol. 17*, 299–313.

Photosensitive DNA Cleavage and Phage Inactivation by Copper(II)–Camptothecin

June Kuwahara, Tadashi Suzuki, Kyoko Funakoshi, and Yukio Sugiura*
Faculty of Pharmaceutical Sciences, Kyoto University, Sakyo-ku, Kyoto 606, Japan
Received July 19, 1985

ABSTRACT: Upon irradiation with 365-nm light, copper(II)–camptothecin significantly produced single- and double-strand breaks of DNA and also induced a marked inactivation of bacteriophage. The nucleotide sequence analysis exhibited considerably random DNA cleavage. The DNA strand scission by the camptothecin–Cu(II)–UV light system, as well as the phage inactivation, was strongly suppressed by bathocuproine and catalase, indicating participation of cuprous species and hydrogen peroxide in the reaction. The present results suggest that (1) Cu(II) ion may play an important role as a cofactor in antitumor action of camptothecin and (2) the combination of copper–camptothecin plus long-wave ultraviolet light is useful against certain cancer treatment as a new photochemotherapy.

Camptothecin (CPT) isolated from *Camptotheca acuminate* (Nyssaceae), a tree widely distributed in the sourthern part of China, is a typical cytotoxic alkaloid and has some therapeutic effects on gastric, rectum, and bladder tumors (Cai & Hutchinson, 1983; Wall & Wani, 1980). Although CPT exhibits dose-dependent toxic side effects, the 10-hydroxy derivative of the compound has been clinically used in the cancer treatment in the People's Republic of China with considerable success against liver carcinoma and head–neck cancer. In Japan, the clinical evaluation of CPT derivatives as an antineoplastic agent has been actively continued.

The alkaloid inhibits nucleic acid synthesis rather than protein synthesis, and its rapid suppression of the former is probably responsible for the cytotoxic action of CPT (Cai & Hutchinson, 1983; Wall & Wani, 1980). In contrast with the DNA synthesis, the RNA synthesis is immediately restored

0006-2960/86/0425-1216$01.50/0

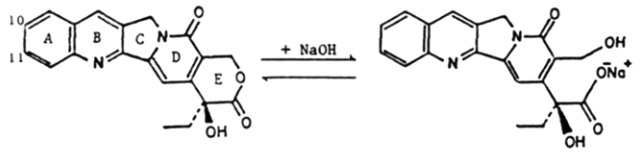

camptothecin camptothecin sodium salt
(Na-camptothecin)

FIGURE 1: Structure of camptothecin.

to the original level by the removal of CPT from the medium. Indeed, the addition of CPT to HeLa cells or adenovirus-infected HeLa cells results in the partial degradation of cellular and viral DNAs (Horwitz & Horwitz, 1971). Fukada (1980) also observed that this alkaloid interacts with closed-circular SV40 DNA to induce an alkali-labile linkage in the E strand. Therefore, the cell target sites of CPT are presumably DNA. It is uncertain whether the antitumor activity of CPT is due to an intercalation (Wall & Wani, 1980), a bioreductive alkylation (Moore, 1977), or a free-radical (Lown & Chen, 1980) mechanism toward cellular DNAs.

Camptothecin has an extended π-electron system and is a photosensitive molecule. Certain transition metals such as Fe(II) and Cu(II) are known to accelerate DNA strand scission induced by anticancer drugs bleomycin and streptonigrin (Sugiura et al., 1985, 1984). Therefore, photosensitization of the CPT–metal complex system may effectively generate radicals to attack DNA. This work has been promoted also by the findings that some metal complexes of bleomycin (Suzuki et al., 1985a) and 4,7-diphenyl-1,10-phenanthroline (Barton & Raphael, 1984) cleave DNA in the presence of light.

Herein, we found, first, remarkable photosensitive DNA strand scission and bacteriophage inactivation of copper(II)–CPT and also examined the molecular mechanism of these phenomena. The present results clearly demonstrate significant effect of photoactivated CPT–Cu(II) complex on DNA and utility of the combination of copper–CPT plus long-wave ultraviolet light against certain cancer treatment. The structure of camptothecin is given in Figure 1.

Experimental Procedures

Purified camptothecin (CPT) was kindly supplied by Yakult Co. Ltd. (Tokyo). Catalase (bovine liver; 3000 units/mg) and superoxide dismutase (bovine blood; 3000 units/mg) were purchased from Sigma Chemicals Co. Calf thymus DNA and 4,7-diphenyl-2,9-dimethyl-1,10-phenanthroline (bathocuproine) were obtained from P-L Biochemicals and Dojin Chemicals, respectively. All other reagents used were of commmercial reagent grade. The labwares were acid-washed and thoroughly rinsed in order to avoid contamination by foreign metal ions, and also fully deionized water was used throughout the experiments.

The DNA cleavage activity was determined on purified ϕX174 RF or pBR322 DNAs by using 1% agarose gel electrophoresis which contained ethidium bromide (0.5 μg/mL). Typical reaction mixtures including 20 mM borate buffer (pH 7.6) and 500 ng of DNA were treated, as indicated in the captions of Figures 2 and 3, with 20 or 50 μM Cu(II)–CPT plus a 365-nm light system under aerobic conditions. The reaction samples were incubated at 20 °C for 60 or 120 min. After the DNA was precipitated by addition of cold ethanol, each sample was dissolved in 20 μL of glycerol (10%) containing bromophenol blue dye (0.05%). The gel electrophoresis was carried out at 150 V and 40 mA.

A restriction fragment of 396 base pairs was obtained by digestion of the ϕX174 RF DNA with the restriction endonuclease *Hpa*II. After the incubation with bacterial alkaline phosphatase the 5′ ends were labeled with ^{32}P by treatment with bacteriophage T4 polynucleotide kinase and [γ-^{32}P]ATP, and this doubly end-labeled DNA fragment was digested with *Hae*III. The singly end-labeled 249-base-pair fragment was isolated by preparative 5% polyacrylamide gel electrophoresis. The CPT–Cu(II) complex in the buffer was added to the solution containing the ^{32}P-labeled DNA piece and sonicated calf thymus carrier DNA (1 μg). The reaction samples (50 μL) were irradiated at a distance of 10 cm from the UV lamp (15 W) emitting mainly 365-nm light at 20 °C for 1.4 h. After 0.2 M ethylenediaminetetraacetic acid (EDTA) (5 μL) was added to stop the reaction, the DNA was precipitated with cold ethanol, dried, and dissolved in the loading buffer (5 μL) containing 10 mM NaOH, 1 mM EDTA, 0.1% xylene cyanol, and 0.1% bromophenol blue. The DNA was denatured by heating at 90 °C for 1 h before transferring to the gel, and then the DNA samples were subjected to electrophoresis together with the standard sequencing fragments (Maxam & Gilbert, 1980) on a 10% polyacrylamide/7 M urea slab gel. The electrophoresis was performed at 1500 V for 4.5 h.

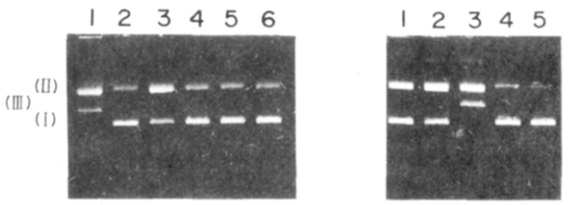

FIGURE 2: Agarose (1%) gel elecrophoretic patterns of ethidium bromide stained ϕX174 RF (left) and pBR322 (right) DNAs after treatment with camptothecin (CPT)–Cu(II) (1:1) complex. (Left) The samples contained 0.5 μg of ϕX174 RF DNA, 20 mM borate buffer (pH 7.6), and the following additions: lanes 1 and 2, 20 μM Cu(II)–CPT; lane 3, 20 μM CPT; lane 4, 20 μM Cu(II); lanes 5 and 6, none. The reaction mixtures were incubated at 20 °C for 60 min in the dark (lane 2) or under 365-nm light irradiation (lanes 1 and 3–5), and lane 6 represents the DNA control. The UV irradiation was performed at a distance of 10 cm from the UV lamp to the sample. (Right) The samples contained 0.5 μg of pBR322 plasmid DNA, 20 mM borate buffer (pH 7.6), and the following additions: lane 1, 50 μM Cu(II); lane 2, 50 μM CPT; lane 3, 50 μM Cu(II)–CPT; lanes 4 and 5, none. The reaction mixtures were incubated at 20 °C for 120 min under 365-nm light irradiation (lanes 1–4), and lane 5 represents the DNA control. The UV irradiation was performed at a distance of 20 cm for the UV lamp to the sample.

Bacteriophage ϕX174 am3 was prepared as reported previously (Fukada & Sinsheimer, 1976), and *Escherichia coli* HF4714 was used as the indicator bacteria of the phage. The reaction samples containing 1×10^6 plaque-forming units/mL phage ϕX174 am3 were treated, as indicated in the caption of Figure 8. The survival of the phage was assayed by a double agar technique (Adams, 1959), and the survival ratio (percent) was estimated by comparing the numbers of plaque-forming units with those at zero time. Single-strand DNAs from ϕX174 am3 particles were extracted by a hot phenol method (Guthrie & Sinsheimer, 1963) after the treatment with the CPT–Cu(II)–UV light and some control systems. The change of DNA forms in the phage particles was analyzed by using 2% agarose gel electrophoresis that contained 0.5 μg/mL ethidium bromide.

X-Band ESR and electronic absorption spectra were measured with a JES-FE-3X spectrometer at 77 K and a Hitachi 330 spectrophotometer at 20 °C, respectively.

Results

Figure 2 (left) shows typical gel electrophoretic patterns of covalently closed-circular (form I) ϕX174 RF DNA treated

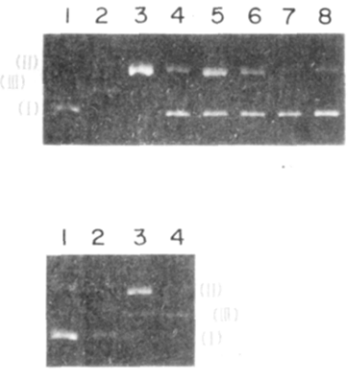

FIGURE 3: Agarose (1%) gel electrophoretic patterns of ethidium bromide stained ϕX174 RF DNA after treatment with the CPT–Cu(II) complex in the presence of bathocuproine (upper) or catalase (lower). (Upper) The samples contained 0.4 μg of ϕX174 RF DNA, 20 mM borate buffer (pH 7.6), and the following additions: lane 1, none; lane 2, 50 μM Cu(II)–CPT; lane 3, 50 μM Cu(II)–CPT plus 10 μM bathocuproine; lane 4, 50 μM Cu(II)–CPT plus 100 μM bathocuproine; lane 5, 50 μM CPT; lane 6, 50 μM CPT plus 100 μM bathocuproine; lane 7, 50 μM Cu(II); lane 8, 50 μM Cu(II) plus 100 μM bathocuproine. The reaction solutions of lanes 2–8 were irradiated with 365-nm light at 20 °C for 60 min. (Lower) The samples contained 0.4 μg of ϕX174 RF DNA, 20 mM borate buffer (pH 7.6), and the following additions: lane 1, none; lane 2, 50 μM Cu(II)–CPT plus 10 μg/mL catalase; lane 3, 50 μM Cu(II)–CPT plus 10 μg/mL boiled catalase; lane 4, 50 μM Cu(II)–CPT. After the reaction, solutions of lanes 2–4 were irradiated with 365-nm light at 20 °C for 60 min, each sample was treated with phenol, and then the DNA was precipitated by cold ethanol.

with the photoactivated CPT–Cu(II) complex system (lane 1). In marked contrast with some controls (lanes 2–6), the Cu(II)–CPT system significantly caused single- and double-strand breaks of DNA to form nicked circular (form II) and linear (form III) duplexes by the irradiation of 365-nm light. Under the same experimental conditions, the CPT–Cu(II) complex in the dark (lane 2), Cu(II) plus UV light (lane 4), and DNA plus UV light (lane 5) had little DNA breakage activity. The CPT plus UV light system (lane 3) induced a slight increase in nicked circular DNA, as Lown and Chen (1980) previously reported. However, its effect was much lower than that of the CPT–Cu(II)–UV light system. Similar remarkable DNA strand scission by the photoactivated CPT–Cu(II) complex was also observed in the experiments of plasmid pBR322 DNA instead of phage ϕX174 RF DNA [see Figure 2 (right)]. In addition, the replacement of borate buffer (pH 7.6) by Tris buffer (pH 7.2) gave no changes on the present DNA cutting. The DNA cleavage of the CPT–Cu(II)–UV light system at 0 °C was considerably lower than that at 20 °C.

The effects of bathocuproine and catalase on the DNA cleavage reaction by the CPT–Cu(II)–UV light system are clearly presented in Figure 3. The conversion to form III DNA decreased with increasing concentration of bathocuproine, and the DNA strand scission was almost perfectly inhibited by the addition of 100 μM bathocuproine. Native catalase also suppressed strongly the DNA degradation of the CPT–Cu(II) complex plus 365-nm light irradiation. In contrast, boiled catalase, superoxide dismutase, 1,4-diazabicyclo[2.2.2]octane, and mannitol had little blocking effect on the DNA breakage. The results suggests that Cu(I) produced during the light activation of the CPT–Cu(II) complex and subsequent formation of active oxygen radicals, in particular hydrogen peroxide, may be responsible for the present DNA degradation. In the DNA strand scission by the 1,10-phenanthroline–copper complex system, Sigman and his collaborators have reported that the formation of a peroxy

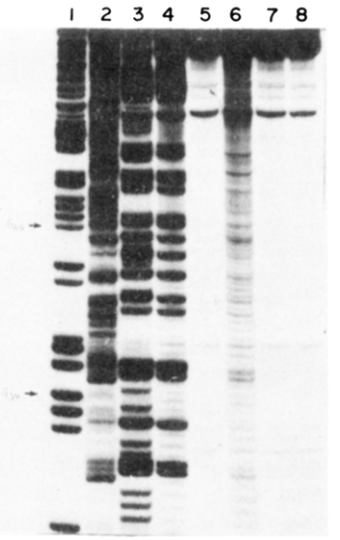

FIGURE 4: Autoradiogram of 10% polyacrylamide/7 M urea slab gel electrophoresis showing the cleavage of the 249-base-pair ϕX174 RF DNA fragment by the photoactivated CPT–Cu(II) complex. The reaction mixtures contained 20 mM borate buffer (pH 7.6), 5′-end ^{32}P-labeled DNA piece, 1 μg of carrier calf thymus DNA, and the following additions: lane 5, 20 μM CPT plus 10 μM Cu(II); lane 6, 100 μM CPT plus 50 μM Cu(II); lane 7, 100 μM CPT; lane 8, 50 μM Cu(II). The samples of lanes 5–8 were incubated at 20 °C for 1.4 h under the irradiation of 365-nm light. Lanes 1–4 show the Maxam–Gilbert sequencing reactions for G, A>C, C+T, and C, respectively. The numbers on the left of the figure represent the length of the DNA base fragment from the ^{32}P-labeled *Hpa*II site.

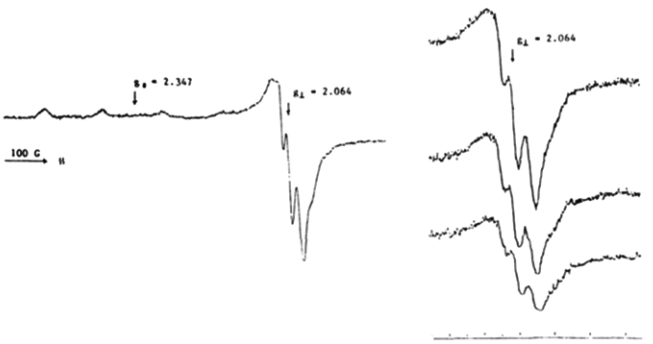

FIGURE 5: ESR spectra for the CPT–Cu(II) complex (left) and for the time course by 365-nm light irradiation (right). The 1:1 CPT–Cu(II) complex was prepared by mixing 2 mM CPT and 2 mM cupric nitrate in borate buffer (pH 7.6) and irradiated with a 365-nm UV lamp at 20 °C for 0, 0.5, and 2.5 h, respectively.

cuprous phenanthroline intermediate is essential (Marshall et al., 1981, 1982).

Figure 4 demonstrates the nucleotide sequence modes on the 249-base-pair ϕX174 RF DNA fragment cleaved by the CPT–Cu(II)–UV light system, together with those by some control systems. Copper(II) ion dramatically enhanced the DNA cleaving activity of the photoactivated CPT, consistent with the result of the experiment using covalently closed-circular DNA. Although almost all bases were degraded in the present DNA cleavage, closer examination revealed that the somewhat preferred breakage sites were the cytosine bases located at the 3′ side of the adenine bases such as TAC̲GC-(5′→3′) and AAAC̲AC̲TGAC̲(5′→3′) sequences. Similar preferred cleavages at the cytosine bases were also detected on two GAC̲GGT(5′→3′) and one GAC̲AC̲ATGC(5′→3′) sequences of the 252-base-pair pBR322 (*Hin*fI–*Rsa*I) fragment. The alteration of nucleotide sequence patterns of the CPT–Cu(II) complex plus UV-light system was hardly observed in the range of 0.1–3.3 drug/base ratio. The relative

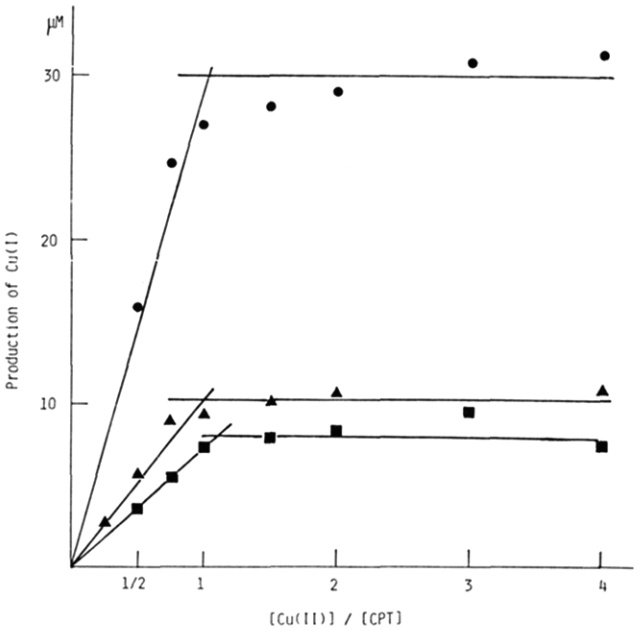

FIGURE 6: Stoichiometric titration of Cu(II)/CPT for Cu(I) production by UV irradiation. At pH 7.6, 10 mM bathocuproine was added to the samples containing various amounts of Cu(II) and 10 (■), 20 (▲), or 50 (●) μM CPT. The reaction solutions were irradiated with the 365-nm light at 20 °C for 3 h.

strong bands at T(34), C(36), and G(49) bases in lanes 5–8 are likely to be due to nicks of the DNA itself.

Figure 5 exhibits the ESR spectra for the 1:1 CPT–Cu(II) complex at pH 7.6 and for the time course by the irradiation of 365-nm light. The ESR features are characteristic of pseudo-square-planar Cu(II) configuration. The present ESR parameters ($g_{\parallel}$ = 2.347, $g_{\perp}$ = 2.064, and $A_{\parallel}$ = 14.5 mK), which are close to those ($g_{\parallel}$ = 2.362, $g_{\perp}$ = 2.078, and $A_{\parallel}$ = 14.7 mK) of the 1:1 triglycylglycine–Cu(II) complex at pH <4 (Falk et al., 1967), reveal oxygen donor sets of the Cu(II)-coordination site. Therefore, the copper ion may interact with the oxygen atoms of α-hydroxy lactone in the E ring of camptothecin. With the UV irradiation of the CPT–Cu(II) complex for 0.5 and 2.5 h, the ESR signals of Cu(II) were decreased to 72% and 48%, respectively, suggesting the reduction from Cu(II) to Cu(I). We also examined colorimetrically the Cu(I) production using bathocuproine, a Cu(I)-specific chelator. The 365-nm light irradiation effectively induced the formation of Cu(I) in the CPT–Cu(II) complex. By the irradiation for 0.5 and 3 h, the 50 μM CPT–Cu(II) complex gave 5.78 and 26.7 μM of Cu(I), that is, the Cu(II) residues of 88% and 47%, respectively. These values were approximately corresponding to the estimation from the ESR measurements. In the absence of CPT, the UV light induced no significant reduction of free curpic ion under the same experimental condition.

Figure 6 represents the job plot for Cu(I) concentration calculated by the bathocuproine method vs. the Cu(II)/CPT molar ratio. The UV irradiation of the 1:1 CPT–Cu(II) complex was performed for 3 h. The controls of CPT–bathocuproine–UV and Cu(II)–bathocuproine–UV systems showed little absorptions at 480 nm. At the Cu(II)/CPT molar ratio of 1/1, the Cu(I) production became to be approximately constant. Similarly, the effect of molar ratio of CPT/Cu(II) on the present DNA strand scission is shown in Figure 7.

Figure 8 indicates the influence of the CPT–Cu(II)–UV light system on the inactivation of bacteriophage φX174 am3.

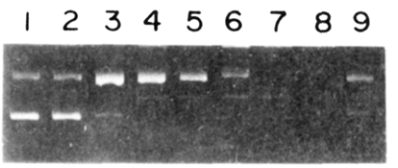

FIGURE 7: Effect of the CPT/Cu(II) ratio on DNA strand scission by the CPT–Cu(II)–UV light system. The samples contained 0.56 μg of φX174 RF DNA, 20 μM Cu(II), 20 mM borate buffer, and the following additions: lane 3, 5 μM CPT; lane 4, 10 μM CPT; lane 5, 15 μM CPT; lane 6, 20 μM CPT; lane 7, 40 μM CPT; lane 8, 60 μM CPT. Lanes 1, 2, and 9 were the controls of 0.56 μg of DNA, 20 μM Cu(II), and 60 μM CPT, respectively. After the irradiation with 365-nm light at 20 °C for 90 min, the electrophoresis of the samples was performed by using 1% agarose gel containing ethidium bromide (0.5 μg/mL).

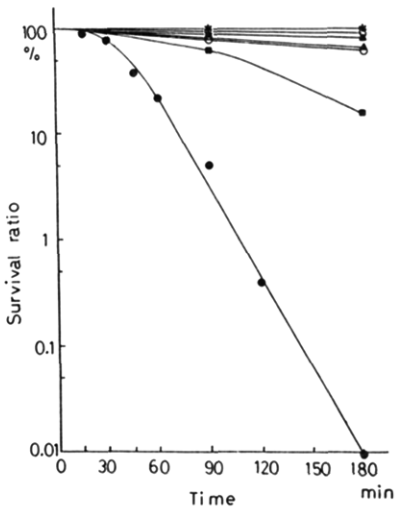

FIGURE 8: Inactivation of phage φX174 am3 by the CPT–Cu(II)–UV light system. The reaction mixtures (total volume 0.2 mL) contained 20 mM borate buffer (pH 7.6), 1 × 10^6 plaque-forming units/mL φX174 am3, and the following additions: 100 μM CPT and 10 μM Cu(II) (●); 100 μM CPT (■); 10 μM Cu(II) (▲); none (asterisk). The samples were irradiated with a high-pressure mercury lamp (500 W) at 20 °C for the indicated times. Dark controls containing 100 μM CPT and 10 μM Cu(II) (○), 100 μM CPT (□), and 10 μM Cu(II) (△) were incubated at 20 °C for the indicated times under dark conditions.

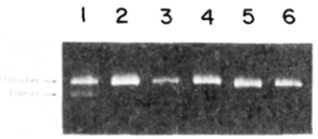

FIGURE 9: Induction of DNA strand scission in phage φX174 am3 particles by the CPT–Cu(II)–UV light system. Single-strand DNAs were extracted by a hot phenol method from reaction mixtures that contained 20 mM borate buffer (pH 7.6), 4 × 10^{11} plaque-forming units/mL, and the following additions: lanes 1 and 2, 100 μM CPT and 50 μM Cu(II); lane 3, 100 μM CPT; lane 4, 50 μM Cu(II); lanes 5 and 6, none. The samples of lanes 1 and 3–5 were irradiated with a high-pressure mercury lamp (500 W) at 20 °C for 2 h, and the samples of lanes 2 and 6 were incubated at 20 °C for 2 h under dark conditions.

When the phage was irradiated with a high-pressure mercury lamp in the presence of the CPT–Cu(II) complex, the infection of phage φX174 am3 remarkably decreased. By contrast, some control systems such as CPT–UV light and Cu(II)–UV light were evidently less effective. The similar phage inactivation was also obtained by irradiation of a UV lamp emitting mainly 365-nm light, instead of a high-pressure mercury lamp. The combination of the CPT–Cu(II) complex and UV light gave significant damage on the bacteriophage consisting of single-strand DNA and proteins. Figure 9 demonstrates the

gel electrophoretic patterns of ϕX174 am3 single-strand DNAs extracted from the phage particles after the treatment of these reaction systems. Indeed, the CPT–Cu(II)–UV light system clearly stimulated the DNA strand breaks in the ϕX174 am3 particles to form linear DNA. This result strongly suggests that the phage inactivation induced by the CPT–Cu(II)–UV light system is attributed to the DNA cleavage reaction. As well as the strand scission of isolated double-strand DNA, the present phage inactivation was powerfully inhibited by catalase and bathocuproine (data not shown).

Discussion

Although photoactivated camptothecin induced only a weak single-strand break of the DNA chain, the significant double- and single-strand breaks were stimulated in the presence of copper(II) ion. The effective concentration for the present DNA cleavage by the CPT–Cu(II) complex (20 μM) was clearly lower than that of the 4′-(*p*-acridinylamino)-methanesulfon-*m*-anisidide–Cu(II) complex (100–250 μM) which causes a single-strand break of DNA (Wong et al., 1984). Of special interest is the fact that the DNA cleavage activity of the CPT–Cu(II)–UV light system was comparable to that of the 1,10-phenanthroline–copper complex system, a typical DNA-cleaving system (Sigman et al., 1979). In addition, the CPT–Cu(II)–UV light system showed high activity for the phage inactivation which is substantially associated with the DNA strand scission. Under the same experimental condition, the DNA breakage activity and phage inactivation ability of other transition metal–CPT complexes were carefully tested. The effects of Mn(II), Fe(II), Co(II), Ni(II), Zn(II), Fe(III), and Co(III) were negligibly small and comparable to the controls. Therefore, the present results demonstrate copper-specific promotion of the DNA cleavage and phage inactivation by photoactivated CPT. In the antitumor action of CPT of which the biological target is probably DNA, it is of particular importance to propose that the Cu(II) ion may play a significant role as cofactor. Certain metal ions such as Fe(II) and Cu(II) are known to essentially participate in the action mechanisms of anticancer drugs bleomycin and streptonigrin (Sugiura et al., 1985). These antitumor antibiotics also produce prominent DNA strand scission. Indeed, Fe(II) and Cu(II) ions are popular metals in biological systems.

Without the UV irradiation, the CPT–Cu(II) complex has little DNA-breaking and phage-inactivating activities. The Cu(II)–CPT system appears to require an appropriate "activation" instead of UV light in vivo. We investigated the influence of reductions such as NADPH and $Na_2S_2O_4$ on the DNA cleavage and phage inactivation by the CPT–Cu(II) complex system. The effect of reductants was clearly positive, but not as remarkable as that of the UV light. It is likely that reductant alone does not suffice for full activation of the CPT–Cu(II) complex system. In order to exhibit significant activity in vivo, therefore, a process such as metabolic activation may be necessary for CPT or Cu(II)–CPT. Indeed, it is well-known that aflatoxin B_1, a typical DNA-target carcinogen, is also activated by UV light as well as liver microsomal enzyme system (Misra et al., 1983).

The present DNA breakage and phage inactivation reactions were strongly inhibited by catalase and bathocuproine, but not by superoxide dismutase, mannitol, and 1,4-diazabicyclo-[2.2.2]octane. The result suggests that (1) the CPT–Cu(II)–UV light system induces copper redox and oxygen activation and (2) together with cuprous species, hydrogen peroxide rather than superoxide anion radical, hydroxyl radical, and singlet oxygen participates in the DNA cleavage and phage inactivation. Similar strong inhibition of catalase and bathocuproine was also observed in the DNA cleavage by the 1,10-phenanthroline–Cu(I)–molecular oxygen system (Marshall et al., 1981). In this reaction system, the 1,10-phenanthroline–cuprous complex and hydrogen peroxide are essential coreactants. The prominent DNA breakage by UV irradiation has been also detected in the Co(III), Fe(III), and Mn(III) complexes of bleomycin (Suzuki et al., 1985a) and the Co(III) complex of 4,7-diphenyl-1,10-phenanthroline (Barton & Raphael, 1984). However, the bleomycin–copper(I,II) complex shows no significant DNA cleavage activity in the presence of reductant, hydrogen peroxide, or UV light (Suzuki et al., 1985b).

The CPT–Cu(II)–UV light system degraded the isolated DNA fragment somewhat preferentially at some cytosine bases adjacent to adenine bases such as the AAACACT(5′→3′) sequence. In the DNA strand scission of the streptonigrin–Cu(II)–NADPH system, similar preferred cleavage sites were several cytosine bases which are adjacent to guanine bases such as the GCGG(5′→3′) sequence (Sugiura et al., 1984). The ^{1}H NMR evidence revealed the interaction between the pyridine ring of streptonigrin and the purine bases of nucleic acid (Sugiura et al., 1984). The bleomycin–iron complex system shows considerably guanine–pyrimidine (5′→3′) sequence specificity which is attributable to the selective interaction between the bithiazole group of bleomycin and the guanine bases of DNA (Sugiura & Suzuki, 1982). Therefore, the present adenine–cytosine selectivity may suggest an interaction of the quinoline ring of the CPT molecule with the purine rings of DNA. On the other hand, the 1,10-phenanthroline–cuprous complex system exhibits little nucleotide sequence specificity in the DNA cleavage reaction (Carteright & Elgin, 1982).

As seen in Figure 9, the treatment of the CPT–Cu(II)–UV light system for phage ϕX174 am3 particles showed obviously the formation of linear DNA. Other control systems gave no linear DNAs. Under this experimental conditions, the survival ratio of the phage was as follows: CPT–Cu(II)–UV system (0.09%), CPT–UV system (18.2%), Cu(II)–UV system (39.6%), CPT–Cu(II) system (40.1%), and UV system (80.5%). As well as the phage ϕX174 am3 which consists of single-strand DNA, the bacteriophage λ comprised of linear double-strand DNA was also inactivated by the treatment of the CPT–Cu(II)–UV light system. The present phage inactivation is not peculiar to the phage ϕX174 am3 and may be independent of DNA strand forms. In the acridine-sensitized photoinactivation of bacteriophage P22, Bryant and King (1984) observed that the DNA of the damaged particles shows no evidence of double-stranded breaks or cross-linking. By contrast, the present phage inactivation induced by the CPT–Cu(II)–UV light system showed clearly DNA cleavage. Therefore, it is most likely that the strong phage inactivation of the CPT–Cu(II)–UV light system is mainly due to the direct DNA strand scission.

PUVA therapy is known to be a type of photochemotherapy that combines psoralen and long-wave ultraviolet (UVA) irradiation and is used to treat psoriasis, a chronic inflammatory skin disease. Camptothecin is also clinically used for treatment of psoriasis in China. Therefore, the present results indicate that the combination treatment of copper–camptothecin plus UVA light may be useful in destroying certain tumors selectively.

Acknowledgments

We thank Dr. Kazumitsu Ueda, Kyoto University, for his helpful suggestion of phage-inactivation experiments.

REFERENCES
Adams, M. H. (1959) in *Bacteriophage*, pp 450–454, Interscience, New York.
Barton, J. K., & Raphael, A. L. (1984) *J. Am. Chem. Soc. 106*, 2466–2468.
Bryant, J. L., Jr., & King, J. (1984) *J. Mol. Biol. 180*, 837–863.
Cai, J.-C., & Hutchinson, C. R. (1983) in *The Alkaloids: Chemistry and Pharmacology* (Brossi, A., Ed.) Vol. 21, pp 101–137, Academic Press, New York.
Carteright, I. L., & Elgin, S. C. R. (1982) *Nucleic Acids Res. 10*, 5835–5852.
Falk, K.-E., Freeman, H., Jansson, T., Malmström, B., & Vanngard, T. (1967) *J. Am. Chem. Soc. 89*, 6071–6077.
Fukada, A., & Sinsheimer, R. L. (1976) *J. Virol. 17*, 776–787.
Fukada, M. (1980) *J. Biochem. (Tokyo) 87*, 1089–1096.
Guthrie, G. D., & Sinsheimer, R. L. (1963) *Biochim. Biophys. Acta 72*, 290–297.
Horwitz, S. B., & Horwitz, M. S. (1971) *Biochem. Biophys. Res. Commun. 45*, 723–727.
Jain, S. C., Bhandary, K. K., & Sobell, H. M. (1979) *J. Mol. Biol. 135*, 813–840.
Lown, J. W., & Chen, H.-H. (1980) *Biochem. Pharmacol. 29*, 905–915.
Marshall, L. E., Graham, D. R., Reich, K. A., & Sigman, D. S. (1981) *Biochemistry 20*, 244–250.
Marshall, L. E., Reich, K. A., Graham, D. R., & Sigman, D. S. (1982) *J. Biol. Chem. 257*, 12121–12128.
Maxam, A. M., & Gilbert, W. (1980) *Methods Enzymol. 65*, 499–560.
Misra, R. P., Muench, K. F., & Humayun, M. Z. (1983) *Biochemistry 22*, 3351–3359.
Moore, H. W. (1977) *Science (Washington, D.C.) 197*, 527–532.
Sigman, D. S., Graham, D. R., D'Aurora, V. D., & Stern, A. M. (1979) *J. Biol. Chem. 254*, 12269–12272.
Sugiura, Y., & Suzuki, T. (1982) *J. Biol. Chem. 257*, 10544–10546.
Sugiura, Y., Kuwahara, J., & Suzuki, T. (1984) *Biochim. Biophys. Acta 782*, 254–261.
Sugiura, Y., Takita, T., & Umezawa, H. (1985) in *Metal Ions in Biological Systems* (Sigel, H., Ed). Vol. 19, pp 81–108, Marcel Dekker, New York.
Suzuki, T., Kuwahara, J., Goto, M., & Sugiura, Y. (1985a) *Biochim. Biophys. Acta 824*, 330–335.
Suzuki, T., Kuwahara, J., & Sugiura, Y. (1985b) *Biochemistry 24*, 4719–4721.
Wall, M. E., & Wani, M. C. (1980) in *Anticancer Agents Based on Natural Product Models* (Cassady, J. M., & Douros, J. D., Eds.) p 417, Academic Press, New York.
Wong, A., Huang, C.-H., & Crooke, S. T. (1984) *Biochemistry 23*, 2946–2952.

Proton Nuclear Magnetic Resonance Investigation of the Spin-State Equilibrium of the α and β Subunits in Intact Azidomethemoglobin

Saburo Neya* and Noriaki Funasaki
Department of Physical Chemistry, Kyoto Pharmaceutical University, Yamashina, Kyoto 607, Japan
Received September 4, 1985

ABSTRACT: The hyperfine-shifted proton NMR spectra of human azidomethemoglobin were examined at 300 MHz in the 2–60 °C range. From analysis of the temperature-dependent heme methyl shifts, the thermal spin-state equilibria of the α and β subunits were independently analyzed in the intact tetramer. The thermodynamic values of the spin equilibrium of the α and β subunits were comparable, suggesting that the spin equilibrium properties of the constituent subunits are similar to each other. Examination of the azidomethemoglobins reconstituted with deutero- or mesohemin further shows that the α and β subunit difference is still small in these hemoglobins probably due to the smallness of the steric and electronic difference of the heme 2,4-substituents of the examined porphyrins. The similarity of the spin equilibrium profiles of the subunits indicates that the strain imposed from the globin to the heme iron is of comparable magnitude for the α and β subunits within the azidomethemoglobins.

Considerable attention has been paid to the spin state of hemoglobin because a change of iron spin is involved in ligand binding to deoxyhemoglobin. In an effort to investigate the structural alterations by ligand binding, the magnetic properties of hemoglobin have been measured for ferrous (Cerdonio et al., 1985; Savicki et al., 1984) and ferric (Beetlestone & George, 1964; Iizuka & Yonetani, 1970) derivatives. Among the methemoglobin derivatives, azidomethemoglobin, which is in a thermal spin-state equilibrium, has been extensively characterized with Mössbauer (Winter et al., 1972), infrared (McCoy & Caughey, 1970; Alben & Fager, 1972), resonance Raman (Scholler & Hoffman, 1979; Cho et al., 1981), electron spin resonance (Scholler & Hoffman, 1979), and visible absorption (Neya et al., 1983) spectroscopies and magnetic susceptibility measurements (Beetlestone & George, 1964; Iizuka & Kotani, 1969; Philo & Dreyer, 1985; Messana et al., 1978). Although these physical methods reveal the bulk magnetic properties, they do not discern possible differences between the α and β subunits. Observation of the isolated subunits or valency hybrid hemoglobin may provide information for the individual chain, but the iron spin state may be perturbed due to the structural alteration accompanying subunit separation or the heme–heme interaction between the ferrous and ferric subunits.

The proton NMR spectrum of azidomethemoglobin resolves the α- and β-heme methyl protons (Davis et al., 1969; Iizuka

0006-2960/86/0425-1221$01.50/0